Powder Metallurgy and Metal Ceramics, Vol. 48, Nos. 11-12, 2009

RAPID MECHANICALLY ACTIVATED SOLID-STATE SYNTHESIS OF NANOCRYSTALLINE α-Al_2O_3 USING Fe_2O_3 AND Al

M. Bodaghi,[1,4] A. Mirhabibi,[2] and M. Tahriri[3]

UDC 621.762

In this research, we demonstrate rapid mechanochemical synthesis of nanocrystalline α-alumina (α-Al_2O_3) from a starting mixture of hematite (Fe_2O_3) and aluminum (Al). The formation of α-Al_2O_3 nanocrystallites occurs during the solid-state reaction and through the reduction treatment. Also in this paper, effects of milling time on the particle size and lattice strain of nanocrystalline α-Al_2O_3 are investigated. The results indicate that complete reduction is reached only after 2 h of milling in a planetary mill and the crystallite size of obtained α-Al_2O_3 is in general about 12 nm. Also, it is found that increasing the milling time can effectively decrease the nanocrystalline size and increase the lattice strain of α-Al_2O_3. Finally, the experimental results show appropriate homogeneity and dispersion of related nanocrystallites.

Keywords: *nanostructures, solid-state synthesis, scanning electron microscopy, transmission electron microscopy, X-ray diffraction.*

INTRODUCTION

In recent years, significant research efforts have been devoted to developing inorganic nanocrystals because of their potential application in biology, electronics, optics, transport, and information technology. Although several approaches investigated ways of making these nanocrystals, methods of controlling the size, shape, and crystallinity and various parameters affecting the size and shape of these materials still need to be found [1–4].

Alumina powder is a versatile material which can be sintered into useful ceramics with applications in many industries such as heterogeneous catalysis, abrasives, and adsorbents. It is also a known biocompatible material useful in medical devices such as surgical implants [5–10].

In practice, any method capable of producing very fine-grained polycrystalline materials has been employed to synthesize nanostructured alumina. Alumina has been obtained, for example, by vapor phase reaction [11], precipitation [12], sol–gel [13], hydrothermal [14], and combustion methods [15]. Among the many possible alternatives, solid-state reactions (mechanical treatment) have attracted the maximum attention because they permit the relatively low-cost production of large quantities of nanocrystalline phases. A characteristic feature of all solid-

[1]Ceramic Department, Materials and Energy Research Center, Tehran, Iran. [2]Materials Science & Engineering Department, Iran University of Science and Technology, Tehran, Iran. [3]Biomaterial Group, Faculty of Biomedical Engineering (Center of Excellence), Amirkabir University of Technology, Tehran, Iran.

[3]To whom correspondence should be addressed; e-mail: mohammadreza.tahriri@gmail.com.

Published in Poroshkovaya Metallurgiya, Vol. 48, No. 11–12 (470), pp. 30–37, 2009. Original article submitted April 6, 2009.

state reactions is that they involve the formation of product phase(s) at the interfaces of the reactants. Further, growth of the product phase involves diffusion of atoms of the reactant phases through the product phase, which constitutes a barrier layer preventing further reaction. The solid-state reactions initiated by intensive milling in high-energy ball mills could be a good choice for the ceramic powder preparation. An important criterion for intensive milling is the formation of highly dispersed phased materials typical of metal powders or oxide-based materials (mechanical activation) or the formation of a new product because of a solid-state reaction (mechanochemical synthesis) [16, 17]. Intensive milling increases the area of contact between the reactant powder particles due to reduction in particle size and allows fresh surfaces to come into contact. This allows the reduction to proceed without the necessity for diffusion through the product layer. As a consequence, solid-state reactions that normally require high temperatures will occur at lower temperatures during mechanochemical synthesis without any externally applied heat. In addition, the high defect densities induced by intensive milling in high-energy mills favor the diffusion process. Alternatively, the particle refinement and consequent reduction in diffusion distances (due to microstructural refinement) can at least reduce the reaction temperatures significantly, even if they do not occur at room temperature. Further, mechanical treatment of ceramic powders can reduce particle size and enable obtainment of nanostructured powders, which are of the main interest in current trend of miniaturization and integration of electronic components [18, 19].

Nanocrystalline α-Al_2O_3 powders have been synthesized by the method including the mechanical activation of displacement reactions between Al and Fe oxide, e.g. [20–22].

The reaction between Fe_2O_3 and Al is highly exothermic. A self-propagating combustion reaction can be ignited resulting in high temperature and reaction rates. This can result in the melting of Fe product and separation of Fe and Al_2O_3 in some cases [23]. The enthalpies associated with reaction

$$Fe_2O_3 + 2Al \rightarrow Al_2O_3 + 2Fe \quad (1)$$

are as follows: $\Delta H = -851/4$ kJ/mol., $\Delta G = -840$ kJ/mol.

In this paper, we present the results from the synthesis of nanocrystalline α-Al_2O_3 through the reaction between Al and Fe_2O_3 during mechanical milling.

MATERIALS AND METHODS

Powder Synthesis. The reduction experiments were performed in a Fritsch Pulversette 7 planetary mill (high-energy planetary-ball mill). For preparation of α-Al_2O_3, hardened steel vials and balls were used while the powder-to-ball weight ratio was 1 : 30 in the planetary mill. It is notable that from the eleven balls existing in the Fritsch Pulversette 7, two balls had the diameter of 18 mm and the remaining nine balls 15 mm. The loading, unloading, and milling of the powders were carried out in argon atmosphere.

Iron oxide (Merck No. 103924) and aluminum (Merck No. 101056) with the mean particles were used as the starting reagents. A mixture (8.5 g) of these reactants in stoichiometric proportions corresponding to reaction (1) was milled for 1, 2, 3, 5, 20, 30, 40, and 100 h. To ensure an inert atmosphere during milling, the reactants and grinding media were sealed in a vial whilst within a high-purity argon-filled glove-box.

Powder Characterization. The structural evolution of the powders during processing was studied by x-ray diffraction (XRD) with Philips PW 3710. This instrument works with voltage and current settings of 30 kV and 25 mA, respectively, and uses Cu-K_α radiation (0.1540510 nm). For qualitative analysis, XRD diagrams were recorded in the interval $20^\circ \le 2\theta \le 70^\circ$ at a scan speed of 2°/min. The full widths at half-maximum (FWHM) $\delta(2\theta)$ of the XRD lines at angles 2θ, corrected in quadrature for instrumental broadening, have been used to calculate the mean crystallite size d and the root-mean-square strain by modified Williamson–Hall plot [24]. The modified Williamson–Hall plot is a useful tool for graphically demonstrating any *hkl*-dependence of broadening within a particular diffraction pattern. Plotting $B\cos\theta$ versus $\sin\theta$, where B is the instrument-corrected sample broadening, which often leads to a straight line plot. The intercept of this line gives the crystallite size D and the slope yields the microstrain (lattice strain) e.

The powder sample was coated with a thin layer of gold (Au) by sputtering (EMITECH K450X, England), and then the microstructure of the powder sample was observed with a scanning electron microscope (SEM, JEOL 6400) that operated at the acceleration voltage of 15 kV.

Transmission electron microscopy (TEM) technique was used to observe and analyze the morphology and particle size of the as-synthesized powders. A high-resolution transmission electron microscope (HR-TEM) (Model Tecnai-Philips F30, FEI Co, Hillsboro) was used for this purpose. In order to perform TEM analysis, particles were deposited onto Cu grids, which support a carbon film. The particles were deposited onto the support grids by deposition from a dilute suspension in acetone or ethanol and then observed with an HR-TEM.

Differential and thermogravimetric analyses were carried out in a Shimadzu DTA-TGA-50 apparatus. For this purpose, 30 mg of the sample was loaded in an alumina crucible and was heated from room temperature up to 1200°C in argon atmosphere at a heating rate of 20°C/min^{-1}.

RESULTS AND DISCUSSION

X-Ray Diffraction. With a precursor powder containing iron oxide and Al, the reaction sequence includes the aluminothermic reduction of iron oxide as well as the formation of aluminides. Additionally, α-alumina is formed *in situ* as a product from the reaction between the iron oxide and Al.

Figure 1a shows the XRD traces of iron oxide and Al powders that were mechanically activated at various times, ranging from 1 to 100 h. After 1 h of milling, the powders are a mixture of the starting reactant materials characterized by sharp Bragg peaks of Fe_2O_3 and Al. Increasing the mechanical activation time (1 to 2 h) leads to a decrease in peak intensity and broadening of the Bragg reflection observed in Fig. 1a. This phenomenon indicates the refinement of powder crystallites and an increase in atomic level strains. The final products are a mixture of the α-Al_2O_3 phase coexistent with Fe crystals.

Crystallite Size and Lattice Strain. The crystallite size and lattice strain of α-Al_2O_3 calculated from X-ray peak broadening [25] are presented in Fig. 1b and c, respectively. This figure shows the crystallite size of the

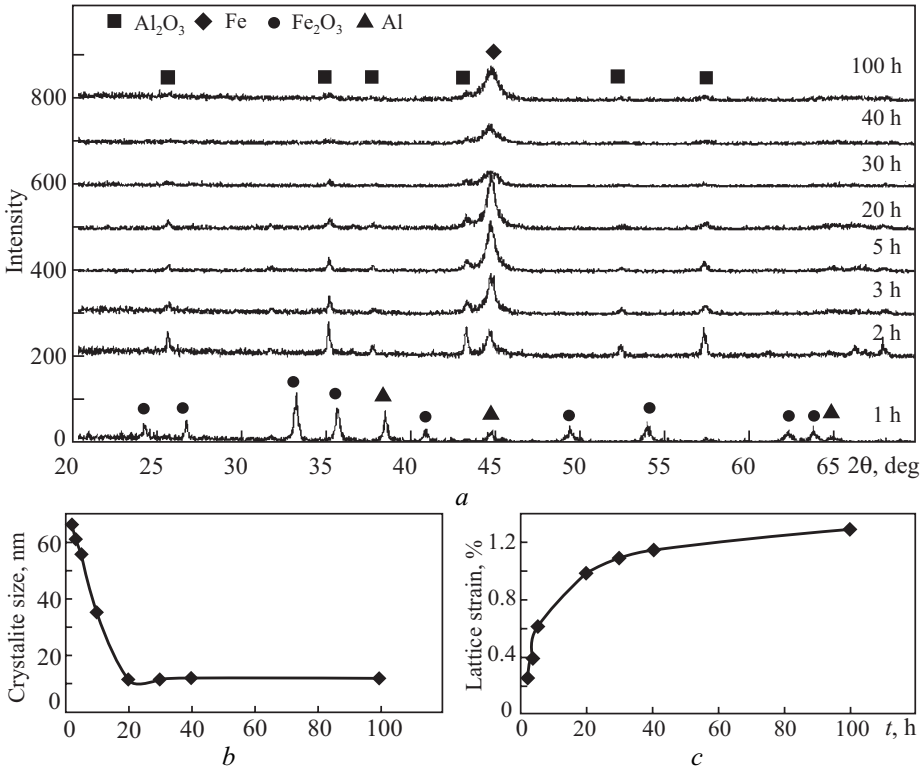

Fig. 1. XRD patterns of samples ball-milled for t = 1 to 100 h (a), crystallite size (*b*), and lattice strain (*c*) of Al_2O_3 in reactively milled samples for t = 1 to 100 h (calculated from X-ray peak broadening)

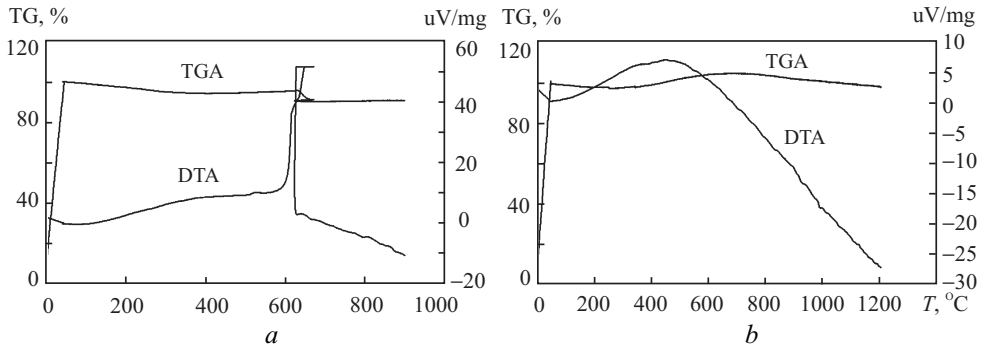

Fig. 2. DTA and TGA curves for (a) unmilled powder and (b) after 2 h of ball milling

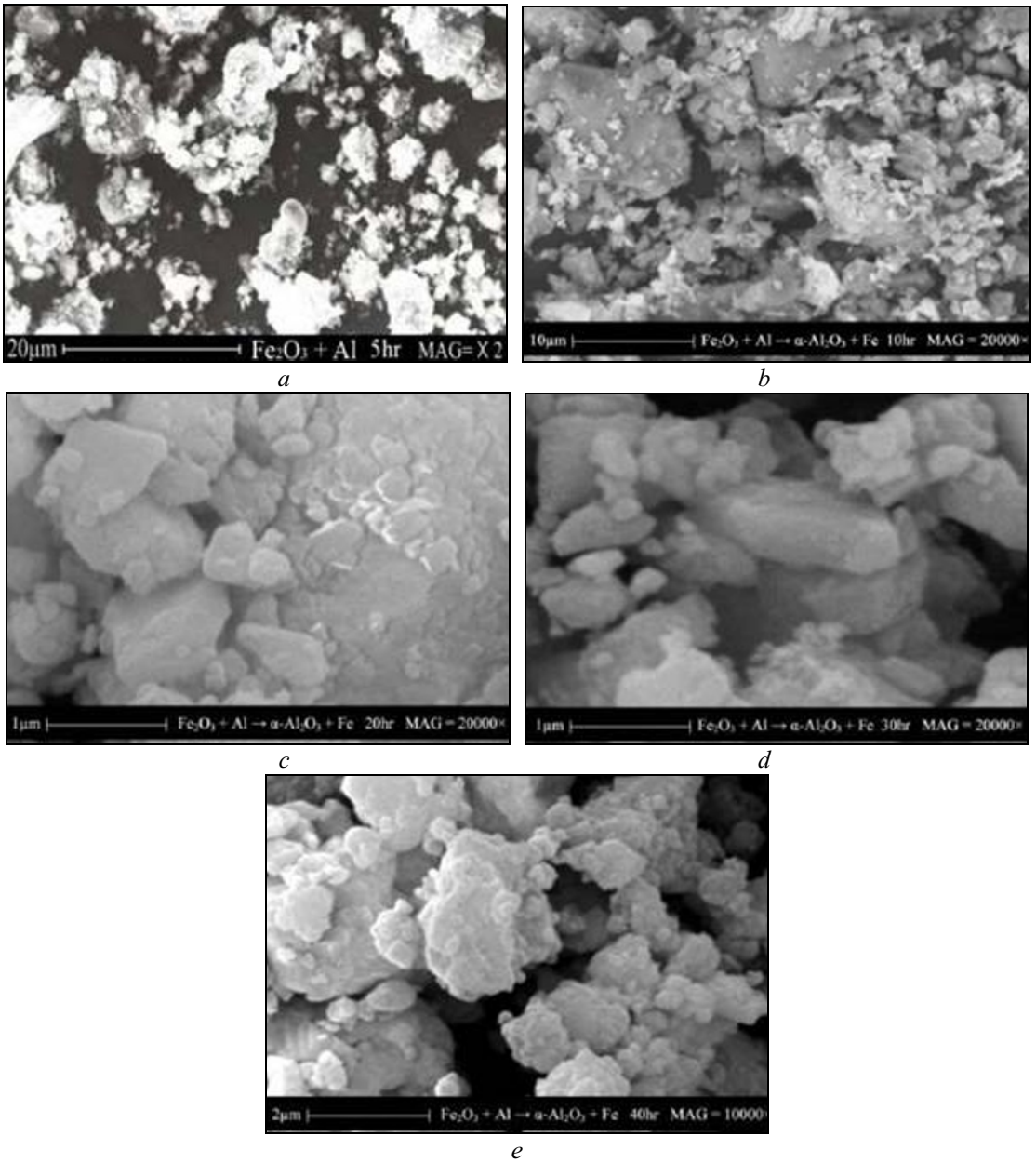

Fig. 3. SEM micrographs (secondary-electron mode) of α-Al_2O_3 + Fe nanocrystalline powder formed after reduction of hematite under mechanical alloying during 5 (*a*), 10 (*b*), 20 (*c*), 30 (*d*), and 40 h (*e*)

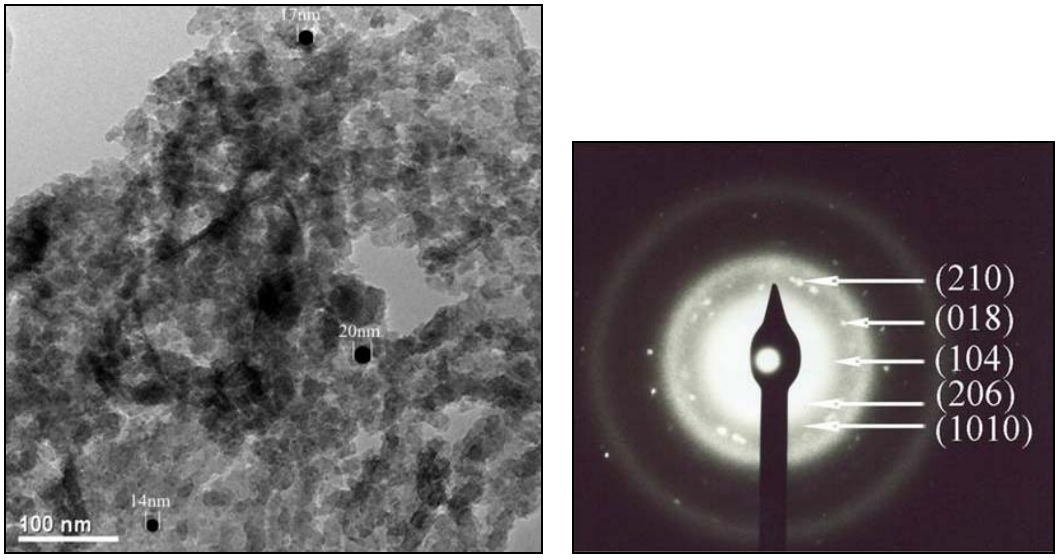

a *b*

Fig. 4. TEM observation of the powder mixtures milled for 20 h after washing with HCl (α-Al_2O_3) (*a*) bright-field TEM micrograph and (*b*) associated SADP

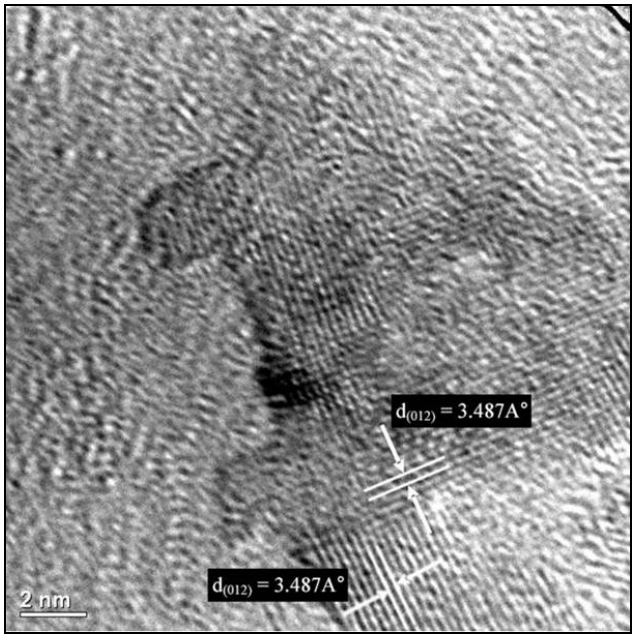

Fig. 5. HR-TEM image of the powder mixture milled for 20 h after washing with HCl (α-Al_2O_3)

obtained α-Al_2O_3 as a function of the mechanical activation time. There is a remarkable decrease in the crystallite size during the initial 20 h of mechanical activation. Then, a further little increase in specific crystallite size is observed when the mechanical activation is extended to 30 and then 100 h by correlating these changes in crystallite size, as a function of activation time, with the phase development, as shown in Fig. 1b. At the initial stage of mechanical activation, refinement in particles and crystallites takes place, whereas the formation of some α-Al_2O_3 nanocrystallites is triggered by mechanical activation. The further increase in the mechanical activation time led to a steady-state reaction, although greater mechanical activation time did no longer refine the particles and crystallites.

Therefore, the average crystallite size of 12 nm was calculated for the α-Al_2O_3 powder that was derived from 20 h of mechanical activation.

Thermal Analysis. A thermal gravimetric analysis of unmilled powder showed that there were no mass changes (<0.05%) during heating up to 1200ºC, confirming the entirely solid-state nature of reactions occurring as expected from [1]. The DTA curves for Fe_2O_3 milled with Al are presented in Fig. 2 for unmilled powder and after 2 h of ball milling times. All the samples were heated to about 1200ºC (first heating run) and cooled to about 25ºC.

With unmilled powders, a sharp endothermic peak appears at about 660ºC, due to the melting of aluminum in the starting material. Then, this melt reacts with Fe_2O_3 powders in the mixture characterized by an exothermic peak which appears above, as shown in Fig. 2a. During the first 2 h of the mechanical activation time, there is no significant peak in the alloy powders, confirming that the reaction is completed after 2 h (Fig. 2b). Therefore, with respect to the thermal analysis results and also XRD analysis results mentioned in the previous section, the process at this stage represents just blending of Al_2O_3 and Fe powders.

Powder Morphology. The SEM micrographs for the milled powders are shown in Fig. 3. The unmilled powder consisted of large rounded grains that were surrounded by smaller submicron grains. The elemental maps confirm that the large grains were aluminum and small grains hematite (Fe_2O_3), as expected from the feed powder particle size. High-magnification image reveals that some small particles were attached tightly to the rough surface of the relatively large particle.

The milled powder showed somewhat different morphology. The grains were comparatively angular consisting of submicron fragments, which appear to have been welded together, forming larger agglomerates. The equilibrium crys-tallite size has been shown to be a typical feature of extended milling [26], although different materials/mixtures have different particle size. It has been noted that the presence of a metallic phase, either added initially or formed by reaction during milling, tends to give a larger particle size than in a metal-free system [27] indicating that metal acts as a binder for the submicron particles.

Figures 4a and b represent a bright-field TEM image and selected-area diffraction pattern (SADP) of the powder after washing with HCl (meaning Al_2O_3). It is mentionable that the process of washing with acid (HCl) was carried out to separate Fe particles from powder mixtures.

In Fig. 4a, the crystallite size of α-Al_2O_3 varies from 12 to 20 nm after milling for 20 h (black rounded shapes). The measured crystallite size of α-Al_2O_3 according to the XRD pattern of the 20 h sample broadening was 12 nm. The selected-area diffraction rings clearly demonstrate that the particles are nanocrystalline. The diffusive rings of the selected-area diffraction pattern (Fig. 4b) suggest that the amorphous structures consist of retained aluminum compounds.

The HR-TEM also confirmed the presence of α-Al_2O_3 in the powder mixture after milling for 20 h. The HR-TEM image of the powder mixture after milling for 20 h (Fig. 5) clearly shows the crystalline walls with reticular distances of 0.3487 nm corresponding to the (0 1 2) face spacing of the α-Al_2O_3 phase.

CONCLUSIONS

In conclusion, we presented fundamental data on the preparation of α-Al_2O_3-based materials by milling of Fe_2O_3 and Al in this research. Nanometer-sized alumina crystallites with a mean size of 12 nm are formed in a planetary mill during 20 h. Also, the steady-state stage of mechanical alloying is reached after milling for 20 h.

Eventually, mechanochemical activation provides precursors of high reactivity. This is the main reason for direct mechanochemical synthesis of α-Al_2O_3 as nanosized crystallites.

REFERENCES

1. S. Bose and S. K. Saha, *Chem. Mater*., 2003, **15**, 4464-4469.
2. M. Bodaghi, A. R. Mirhabibi, H. Zolfonun, et al., *Mater. Res. Innov*., 2008, **12**, 157–161.
3. H. Eslami, M. Solati-Hashjin, and M. Tahriri, *J. Ceram. Process. Res.*, 2008, **9**, 224–229.
4. M. Bodaghi, A. R. Mirhabibi, H. Zolfonun, et al., *Phase Transit*., 2008, **81**, 571–580.
5. K. L. Eckert, M. Mathey, J. Mayer, et al., *Biomaterials*, 2000, **21**, 63–69.
6. P. A. Zieliñski, R. Schulz, S. Kaliaguine, et al., *J. Mater. Res*., 1993, **8**, 2985–2992.

7. L.L. Hench, *J. Am. Ceram. Soc*., 1991, **74**, 1487-1510.
8. N. Travitzky, P. Kumar, K. H. Sandhage, et al., *Mater. Sci. Eng*., 2003, **344A**, 245–252.
9. P. Ganguly and W. J. Poole: *Mater. Sci. Eng.*, 2003, **352A**, 46–54.
10. E. Martínez Flores, J. Negrete, and G. Torres Villaseñor, *Mater. Des*., 2003, **24**, 281–286.
11. C. Suryanarayana, *Prog. Mater. Sci*., 2001, **46**, 1-184.
12. M. Z. Hu and X. Feng, *Encyclop. Nanosci. Nanotech*., 2004, **1**, 687-726.
13. J. Li, Y. Pan, C. Xiang, et al., *Ceram. Int*., 2006, **32**, 587-591.
14. B. Siebert, C. Funke, R. Vaβen, et al., *J. Matter. Process. Tech*., 1999, **92–93**, 195–202.
15. K. Varatharajan, S. Dash, A. Arunkumar, et al., *Mater. Res. Bull*., 2003, **38**, 577–583.
16. J. Xue, D. Wan, S. E. Lee, J et al., *J. Am. Ceram. Soc*., 1999, **82**, 1687-1692.
17. B. D. Stojanovic, A. Z. Simoes, C. O. Paiva-Santos, et al., *J. Euro. Ceram. Soc*., 2005, **25**, 1985–1989.
18. T. Peng, X. Liu, K. Dai, et al., *Mater. Res. Bull*., 2006, **41**, 1638–1645.
19. A. K. Giri, *Adv. Mater*., 1997, **9**, 163–166.
20. P. Matteazzi, G. Le Caer, *J. Am. Ceram. Soc*., 1992, **75**, 2749–2755.
21. J. Ding, T. Ssuzuki, and P. G. McCormick, *J. Am. Ceram. Soc*., 1996, **79**, 2956–2958.
22. C. Cuadrado-Labord, L. C. Damonte, and L. Mendoza-Zelis, *Mat. Sci. Eng*., 2003, **355A**, 106–113.
23. L. Durães, B. F. O. Costa, R. Santos, et al., *Mat. Sci. Eng.*, 2007, **465A**, 199–210.
24. P. Millet and T. Hwang, *J. Mater. Sci*., 1996, **31**, 351-355.
25. P. G. McCormick, *Mater. Trans. J. Japan Inst. Metals*, 1995, **36**, 161–169.
26. S. Schicker, D. E. Garcia, J. Bruhn et al., *Acta Mater*., 1998, **46**, 2485–2492.
27. W. Zeng, A. A. Rabelo, and R. Tomasi, *Key Eng. Mater*., 2001, **189–191**, 16–20.